Electrochemical and Solid-State Letters, **5** (1) A1-A4 (2002)
0013-4651/2001/5(1)/A1/4/$7.00 © The Electrochemical Society, Inc.

Structural Characterization of Mn-Based Materials Using γ-MnOOH Source

Y. S. Lee,[a,*] C. S. Yoon,[b] Y. K. Sun,[c,] and M. Yoshio[a,**,z]**

[a]*Department of Applied Chemistry, Saga University, Saga 840-8502, Japan*
[b]*Division of Material Science and Engineering and* [c]*Department of Chemical Engineering, Hanyang University, Sungdong-gu, Seoul 133-791, Korea*

$LiAl_{0.1}Mn_{1.9}O_4$ and $LiMn_2O_4$ materials were synthesized using LiOH, $Al(NO_3)_3$, and different Mn sources (Mn_3O_4 and γ-MnOOH). X-ray diffraction (XRD) showed that all prepared materials had identical crystalline phase (cubic, $Fd\bar{3}m$). Two materials using the Mn_3O_4 source exhibited different cycling characteristics depending on the cycling voltage range. However, the two materials using the γ-MnOOH source showed an identical cycling performance in both the 3 and 4 V regions. Transmission electron microscope analysis revealed that the materials using γ-MnOOH consisted of two kinds of structures of cubic and tetragonal in the resulting powders although they were shown as a pure cubic spinel structure in the XRD diagram. This indicated a more stable state for the two Mn-based materials using γ-MnOOH when the transformation from the cubic to tetragonal phase occurred in the 3 V region.
 [DOI: 10.1149/1.1419702]

Manuscript submitted June 7, 2001; revised manuscript received September 4, 2001. Available electronically November 8, 2001.

$LiMn_2O_4$ spinel has been widely investigated because of its cost performance, environmental merit, and easy preparation compared with other cathode materials.[1-3] The performance of $LiMn_2O_4$ has been stabilized at room temperature, however, its efficiency at high temperature has been unsatisfactory until now.[4]

Many research groups have reported lots of suggestions which revealed the capacity loss mechanism or improved cycling performance in the 4 V region.[5-8] However, there was no clear suggestion to explain the capacity loss mechanism in the 3 V region except for the Jahn-Teller distortion.[9,10] There has been no report which disputed the Jahn-Teller distortion or revealed unique behaviors in the 3 V region until recently.

However, Sun *et al.* have reported that sulfur-doped spinels, $LiMn_2O_{3.98}S_{0.02}$ and $LiAl_{0.24}Mn_{1.76}O_{3.98}S_{0.02}$ powders, were synthesized by the partial substitution of oxygen in $LiMn_2O_4$, which showed an increased discharge capacity in the 3 V region. These also had excellent cycling performances in the 3, 4, and (3 + 4) V regions.[11,12] Furthermore, Kang and Goodenough reported the synthesis of the $LiMn_2O_4$ material which showed no capacity fading in the 3 V region, even though it was a pure spinel material.[13] Although the two groups failed to perfectly explain why their materials induced their distinct reactions in the 3 V region, note that these results are new observations different from those in previous reports.

We have recently reported the unique cycling characteristics of the $LiAl_{0.1}Mn_{1.9}O_4$ material in the 3 V region. It showed many different characteristics depending on the starting materials and synthetic conditions.[14-16] For instance, we found that $LiAl_{0.1}Mn_{1.9}O_4$ using the Mn_3O_4 source showed a more serious capacity loss than the pure $LiMn_2O_4$ spinel material in the 3 V region, in which the increase in the cubic phase in the $LiAl_{0.1}Mn_{1.9}O_4$ structure prevented a complete structural change from cubic ($Li_{1.0}Mn_2O_4$) to tetragonal ($Li_2Mn_2O_4$) in this voltage region.[14] On the other hand, the $LiAl_{0.1}Mn_{1.9}O_4$ material using the γ-MnOOH source exhibited a better cycling performance than the $LiMn_2O_4$ spinel in both the 3 and 4 V regions. Nevertheless, after 50 cycles the electrode maintained an almost perfect tetragonal phase in the discharged state (~2.2 V).[15]

In this paper, we report the unique structural formation in the $LiAl_{0.1}Mn_{1.9}O_4$ and $LiMn_2O_4$ materials using the γ-MnOOH source and explain the reason why these materials showed stable cycling behavior even in the 3 V region.

Experimental

$LiAl_{0.1}Mn_{1.9}O_4$ and $LiMn_2O_4$ materials were synthesized using LiOH, $Al(NO_3)_3$ and two manganese sources (Mn_3O_4 and γ-MnOOH) by a melt-impregnation method. Each mixture were precalcined at 470 and 530°C for 5 h in O_2 or air, respectively, and then post-calcined at 800°C for 20 h.

The powder X-ray diffraction (XRD, Rint 1000, Rigaku, Japan) using Cu Kα radiation was performed to identify the crystalline phase of the materials. A transmission electron microscope (TEM, JEM 2010, JEOL, Japan) equipped with energy-dispersive X-ray spectrometer (EDS) was employed to characterize the microstructure of the powder. The Li, Al, and Mn concentrations in the resulting materials were analyzed using an inductively coupled plasma spectrometer (ICP, SPS 7800, Seiko Instruments, Japan). To quantitatively test the oxygen content, an oxygen determination analyzer (RO-416DR, EF-40C, LECO Corporation, USA) was used for oxygen analysis.

The electrochemical characterizations were performed using CR2032 coin-type cells. The cathode was 20 mg of accurately weighed active material and 12 mg of conductive binder (8 mg of Teflonized acetylene black (TAB) and 4 mg of graphite). It was pressed on a 250 mm^2 stainless steel mesh used as the current collector at 300 kg/cm^2 and dried at 200°C for 5 h in an oven. This cell consisted of a cathode and a lithium metal anode (Cyprus Foote Mineral Co.) separated by a porous polypropylene film as the separator (Celgard 3401). The electrolyte used was a 1 M $LiPF_6$-ethylene carbonate (EC)/dimethyl carbonate (DMC) (1:2 by volume, Ube Chemical, Japan). The charge and discharge current density was 0.4 mA/cm^2 with a cutoff voltage of 3.0-4.3 V for the 4 V test (2.2-3.6 V for the 3 V test).

Results and Discussion

The $LiAl_{0.1}Mn_{1.9}O_4$ and $LiMn_2O_4$ materials were synthesized using two different manganese sources (Mn_3O_4 and γ-MnOOH). From the XRD pattern in Fig. 1, it seems that all the materials exhibit the same crystalline cubic phase structure without any impurities. However, we found many different characteristics between the two Mn-based materials. We already reported the dissimilar intensity ratio of the (311)/(400) peaks for the $LiAl_xMn_{2-x}O_4$ material using different manganese sources.[17] Furthermore, the intensity ratio of the (311)/(400) peaks for the $LiAl_xMn_{2-x}O_4$ materials using Mn_3O_4 (herein referred to as sample A) showed small values (<1.0) which were lower than those of the $LiAl_xMn_{2-x}O_4$ materials using γ-MnOOH (herein referred to as sample B). Unfortunately, we cannot clearly explain the meaning of this difference; it is assumed that the shape of the (311) and (400) peaks reflects the degree of tetragonal distor-

* Electrochemical Society Student Member.
** Electrochemical Society Active Member.
z E-mail: yoshio@ccs.ce.saga-u.ac.jp

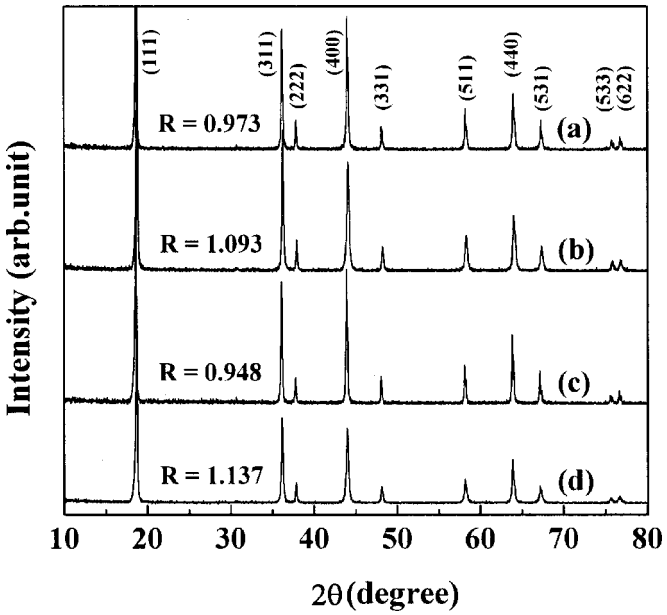

Figure 1. XRD patterns of powders calcined at 800°C in air. (a) $LiAl_{0.1}Mn_{1.9}O_4$ using the Mn_3O_4, (b) $LiAl_{0.1}Mn_{1.9}O_4$ using the γ-MnOOH, (c) $LiMn_2O_4$ using the Mn_3O_4, and (d) $LiMn_2O_4$ using the γ-MnOOH. R is the intensity ratio of the (311)/(400) peaks.

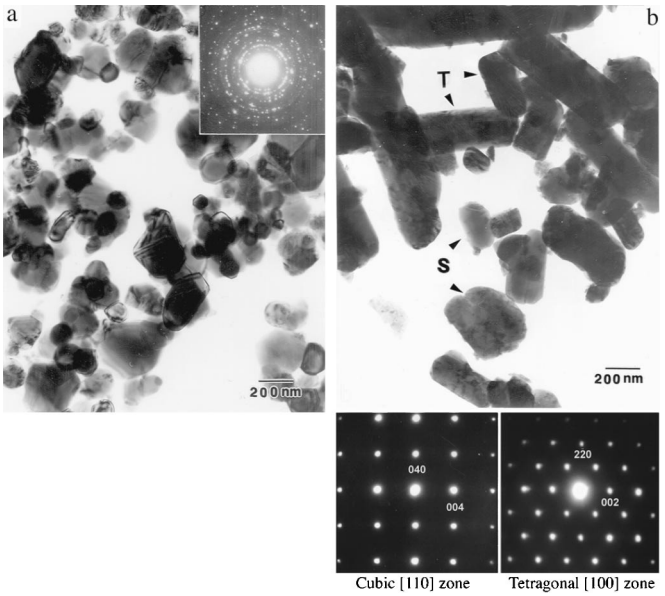

Figure 2. TEM image and SAD pattern of resulting powder before cycling. (a) $LiAl_{0.1}Mn_{1.9}O_4$ using the Mn_3O_4, (b) $LiAl_{0.1}Mn_{1.9}O_4$ using the γ-MnOOH. T: tetragonal, S: cubic.

tion from the cubic spinel structure. To exclude the effect of aluminum, stoichiometric $LiMn_2O_4$ spinels (using Mn_3O_4, sample C; using γ-MnOOH, sample D) were also synthesized under the same synthetic conditions and are shown in Fig. 1c and d, respectively.

Although the XRD results indicated that samples B and D were made with a pure spinel phase, the Rietveld refinement and chemical analysis presented quite different results compared with that of the XRD. As shown in Table I, samples B and D showed different occupation ratios in the oxygen (32e) site. Furthermore, the average manganese valence and oxygen content of these materials were smaller than those of samples A and C.

To find other differences in the structural aspects, a TEM analysis was performed and revealed the same results as the Rietveld and chemical analysis. Figure 2 shows the TEM image of particles for samples A and B. It shows that sample A consisted of 200 nm equiaxed spinel crystals, while sample B had a much larger particle size with a bar-type shape. With further analysis of the powder particles using electron diffraction, it was found that sample A consisted of only a cubic crystal phase as shown in the inset, whereas sample B was composed of multiple phases as shown in the selected area diffraction (SAD) patterns: elongated tetragonal crystals (bar-type shape) and equiaxed cubic crystals (spherical shape). The structure of the elongated particles for sample B was tetragonal with $c/a = 1.2$ and had the [001] preferred growth orientation.

Tabuchi *et al.* also has reported the same result for the $LiMn_2O_4$ material, which has a mixed phase of cubic and tetragonal at room temperature, using the same starting material (LiOH and γ-MnOOH) under similar synthetic conditions.[18] They suggested that the structural difference in $LiMn_2O_4$ using LiOH and γ-MnOOH might have resulted from the different synthetic conditions and starting materials compared to each other. It is also known that a lower symmetry structure for lithium manganese oxide can be prepared by reacting LiOH with γ-MnOOH in a reducing atmosphere although it is not clear how the tetragonal phase was formed during the synthesis process.[19] There is a high possibility that a local deficiency of oxygen has generated the Mn^{3+} (Jahn-Teller) ions during the calcination process which resulted in the tetragonal transformation of the spinel phase as shown in Table I.[20]

Figure 3 shows the variation in the specific discharge capacity with the number of cycles for the different Mn-based materials in the 3 and 4 V regions. We found another unique characteristic from the cycling test results between the two Mn-based materials. In the 4 V region, samples A and B exhibited excellent cycling performance,

Table I. The chemical analyses and atomic positions of the Rietveld refined resulting materials.

Sample (800°C)			$LiAl_{0.1}Mn_{1.9}O_4$		$LiMn_2O_4$	
			Mn_3O_4 (A)	γ-MnOOH (B)	Mn_3O_4 (C)	γ-MnOOH (D)
Occupation ratio	8a site	Li	1.0	1.0	1.0	1.0
		Li	0.007	0.007	0	0
	16d site	Al	0.045	0.045	-	-
		Mn	0.948	0.948	1.0	1.0
	32e site	O	0.984	0.940	0.984	0.977
Coordinate (X,X,X)	32e site	O	0.388	0.389	0.388	0.388
Lattice constant (Å)			8.227	8.223	8.240	8.245
Average Mn valence			3.530	3.515	3.509	3.495
Oxygen content (%)			35.77	33.41	35.23	35.10

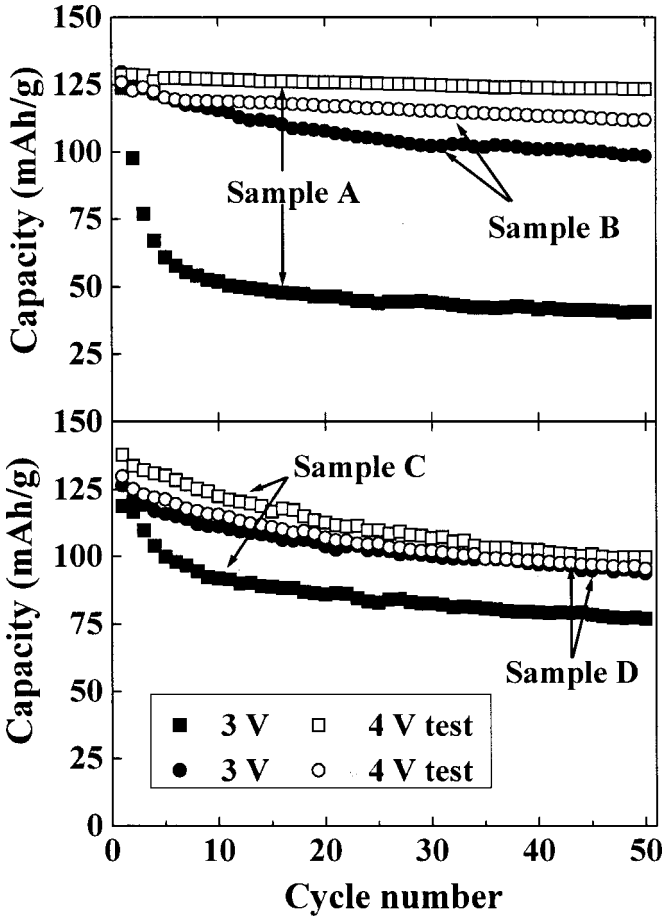

Figure 3. Plot of specific discharge *vs.* number of cycles for the Li/1 M $LiPF_6$-EC/DMC/$LiAl_{0.1}Mn_{1.9}O_4$ and $LiMn_2O_4$ cells in different voltage regions. Cycling was carried out at a constant charge-discharge current density of 0.4 mA/cm^2 between 2.2 and 3.6 V for the 3 V test (3.0 and 4.3 V for the 4 V test).

which resulted from the increased average manganese valence by Al substitution, although there was a difference in the discharge capacity after 50 cycles. Samples C and D also showed good cycling performance in the same voltage region. However, these materials presented quite different cycling behaviors in the 3 V region depending on the manganese source. Sample A showed the lowest discharge capacity and poorest cycling behavior in the 3 V region because of the co-effect of the Jahn-Teller distortion and an unique aluminum effect in the $LiAl_{0.1}Mn_{1.9}O_4$ material using the Mn_3O_4 source as previously reported.[14] Sample C also showed an abrupt capacity loss during the early stage which resulted from the Jahn-Teller distortion, *i.e.* the phase transformation of cubic to tetragonal $Li_2Mn_2O_4$ by lithium insertion in the 3 V region. On the other hand, samples B and D exhibited inimitable cycling behavior in this voltage region. These materials showed almost the same discharge capacity regardless of the Al substitution and did not have any abrupt capacity loss in the early stage. Furthermore, sample D exhibited identical cycling performance in both the 3 and 4 V regions.

On the basis of these results, it was determined that $LiAl_{0.1}Mn_{1.9}O_4$ and $LiMn_2O_4$ using γ-MnOOH source were composed of a mixed phase of cubic and tetragonal, which occurred due to an oxygen deficiency or some other effects during the synthesis. Therefore, this indication might reduce the stress of transformation of the $LiMn_2O_4$ based materials from the cubic to tetragonal phases when the lithium ion is inserted into the 16c site. It is also a natural consideration that it should differentiate the total stress amount by the Jahn-Teller effect between the material with only the cubic phase and with the mixed phase of cubic and tetragonal in the spinel structure. There is a high possibility that some amounts of the tetragonal phase may minimize the volume expansion of the spinel structure because these do not take part in the structural change during the charge/discharge process in the 3 V region, as it retains its original tetragonal phase. Therefore, it should have a high amount of tetragonal phase in the discharged state after 50 cycles and could exhibit a high discharge capacity even with the effect of the Jahn-Teller distortion as observed in our previous report.[15]

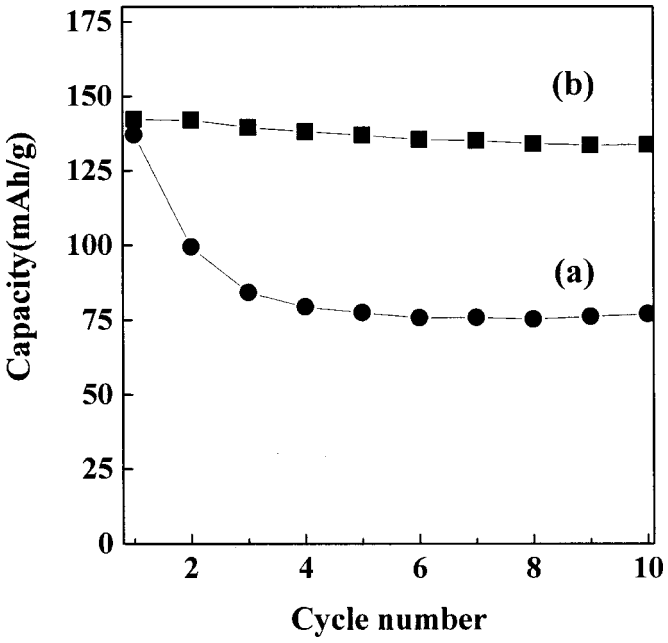

Figure 4. CCCV test in the 3 V region. (a) $LiAl_{0.1}Mn_{1.9}O_4$ using the Mn_3O_4, and (b) $LiAl_{0.1}Mn_{1.9}O_4$ using the γ-MnOOH.

To prove our suggestion in a different way, constant current and constant voltage (CCCV) tests for samples A and B were conducted in the 3 V region. The samples were fully charged/discharged in the voltage range of 2.2 to 3.6 V with the current density of 0.4 mA/cm^2. The processed time was 600 min and the pause time was 10 min. Figure 4 strongly supports our suggestion about the role of the tetragonal phase in the low voltage region. Sample B showed excellent cycling performance until the tenth cycle. The cycle retention rate was 94% in the 3 V region. This means that the lithium insertion/extraction of sample B could proceed with a small amount of Jahn-Teller distortion due to the existence of the tetragonal phase in the spinel structure. However, sample A had an abrupt capacity loss as mentioned above.[14] This is why it is important to obtain good cycling performance of the $LiAl_{0.1}Mn_{1.9}O_4$ and $LiMn_2O_4$ using the γ-MnOOH starting source in the 3 V region.

On the contrary, this indication seems to interfere with the cycling performance in the 4 V region because the structural transformation in this voltage range is the same phase reaction from $LiMn_2O_4$ (cubic) to λ-MnO_2 (cubic). Therefore, samples B and D should have poorer cycling performances than those of samples A and C, which consisted of only the pure cubic phase, in the 4 V region. We could confirm our hypothesis again from the cycling test results as shown in Fig. 3. Sample C showed a higher discharge capacity than sample D up to 50 cycles, moreover, the difference in capacity in the 4 V region between samples A and B was significant because the cubic phase of sample A was intensified by the Al substitution.[15]

From these results, we concluded that $LiAl_{0.1}Mn_{1.9}O_4$ and $LiMn_2O_4$ using the γ-MnOOH have a mixed phase of cubic and tetragonal, whereas $LiAl_{0.1}Mn_{1.9}O_4$ and $LiMn_2O_4$ using the Mn_3O_4 have only the pure cubic phase in the spinel structure. This indication induced a quite different battery performance between the two kinds of Mn-based materials in the 3 V and 4 V region.

Conclusion

$LiAl_{0.1}Mn_{1.9}O_4$ and $LiMn_2O_4$ materials were prepared by the melt-impregnation method using LiOH, $Al(NO_3)_3$ and different Mn sources (Mn_3O_4 and γ-MnOOH). The Mn-based materials using the Mn_3O_4 source showed different cycling performances in the 3 V region. Meanwhile, the two Mn-based material using the γ-MnOOH exhibited similar cycling behaviors in the 3 V region regardless of the Al substitution. A TEM analysis revealed that the materials using the γ-MnOOH consisted of two kinds of structures with cubic and tetragonal phases in the resulting powders although they were shown as a pure cubic spinel structure in the XRD diagram. We conclude that this indication produced the unique electrochemical behavior for the Mn-based material using the γ-MnOOH source in the 3 V region.

Acknowledgment

The authors thank Dr. Okada of Tosoh Co. for powder analysis and technical discussions.

Professor Yoshio assisted in meeting the publication costs of this article.

References

1. J. N. Reimers, E. W. Fuller, E. Rossen, and J. R. Dahn, *J. Electrochem. Soc.*, **140**, 3396 (1993).
2. T. Ohzuku, A. Ueda, and M. Nagayama, *J. Electrochem. Soc.*, **140**, 1862 (1993).
3. J. M. Tarascon, W. R. Mckinnon, F. Coowar, T. N. Bowmer, G. Amatucci, and D. Guyomard, *J. Electrochem. Soc.*, **141**, 1421 (1994).
4. J. Barker, R. Koksbang, and M. Y. Saidi, *Solid State Ionics*, **82**, 143 (1995).
5. D. H. Jang, Y. J. Shin, and S. M. Oh, *J. Electrochem. Soc.*, **143**, 2204 (1996).
6. Y. Xia, Y. Zhou, and M. Yoshio, *J. Electrochem. Soc.*, **144**, 2593 (1997).
7. W. Liu, K. Kowal, and G. C. Farrington, *J. Electrochem. Soc.*, **143**, 3590 (1996).
8. M. M. Thackeray, Y. Shao-Horn, A. J. Kahaian, K. D. Kepler, E. Skinner, J. T. Vaughey, and S. A. Hackney, *Electrochem. Solid-State Lett.*, **1**, 7 (1998).
9. M. M. Thackeray, P. G. David, P. G. Bruce, and J. B. Goodenough, *Mater. Res. Bull.*, **18**, 461 (1983).
10. J. Barker, R. Koksbang, and M. Y. Saidi, *Solid State Ionics*, **82**, 143 (1995).
11. Y. K. Sun, Y. S. Jeon, and H. J. Lee, *Electrochem. Solid-State Lett.*, **3**, 7 (2000).
12. Y. K. Sun and Y. S. Jeon, *Electrochem. Commun.*, **1**, 597 (1999).
13. S. H. Kang and J. B. Goodenough, *J. Electrochem. Soc.*, **147**, 3621 (2000).
14. Y. S. Lee and M. Yoshio, *Electrochem. Solid-State Lett.*, **4**, A85 (2001).
15. Y. S. Lee, H. J. Lee, and M. Yoshio, *Electrochem. Commun.*, **3**, 20 (2001).
16. Y. S. Lee and M. Yoshio, *Electrochem. Solid-State Lett.*, **4**, A155 (2001).
17. Y. S. Lee, N. Kumada, and M. Yoshio, *J. Power Sources*, **96**, 376 (2001).
18. M. Tabuchi, C. Masquelier, H. Kobayashi, R. Kanno, Y. Kobasashi, T. Akai, Y. Maki, H. Kageyama, and O. Nakamura, *J. Power Sources*, **68**, 623 (1997).
19. M. M. Thackeray, *Prog. Solid State Chem.*, **25**, 55 (1997).
20. A. Yamada, K. Miura, K. Hinokuma, and M. Tanaka, *J. Electrochem. Soc.*, **142**, 2149 (1995).